CD8+ T Cells Mediate Viral Clearance and Disease Pathogenesis during Acute Hepatitis B Virus Infection†

Robert Thimme,[1]‡ Stefan Wieland,[1] Carola Steiger,[1] John Ghrayeb,[2] Keith A. Reimann,[3] Robert H. Purcell,[4] and Francis V. Chisari[1]*

Department of Molecular and Experimental Medicine, The Scripps Research Institute, La Jolla, California[1]; Centocor, Malvern, Pennsylvania[2]; Division of Viral Pathogenesis, Beth Israel Deaconess Medical Center, Boston, Massachusetts[3]; and Hepatitis Viruses Section, Laboratory of Infectious Diseases, National Institutes of Health, Bethesda, Maryland[4]

Although the CD4+- and CD8+-T-cell responses to the hepatitis B virus (HBV) are thought to be crucial for the control of HBV infection, the relative contribution of each T-cell subset as an effector of viral clearance is not known. To examine this question, we monitored the course of HBV infection in control, CD4-depleted, and CD8-depleted chimpanzees. Our results demonstrate that CD8+ cells are the main effector cells responsible for viral clearance and disease pathogenesis during acute HBV infection, and they suggest that viral clearance is mediated by both noncytolytic and cytolytic effector functions of the CD8+-T-cell response.

The cellular immune response is thought to play a critical role in viral clearance and disease pathogenesis during hepatitis B virus (HBV) infection (5). Indeed, several studies have shown that the peripheral blood CD4+ helper T-lymphocyte response and the CD8+ cytotoxic T-lymphocyte response to HBV are polyclonal and multispecific in patients with acute viral hepatitis (3, 4, 25, 27, 32, 36). In contrast, the T-cell response is relatively weak in patients with chronic HBV infection, except during spontaneous disease flares or alpha interferon (IFN-α)-induced recovery, when it is easily detectable (31, 33). Furthermore, HBV-specific T cells are detectable in the livers of chronically infected patients, suggesting that they probably contribute to disease pathogenesis, but for functional and/or quantitative reasons, they are unable to terminate the infection (2, 7, 24, 30).

Studies with HBV transgenic mice revealed that, in addition to causing viral hepatitis, HBV-specific CD4+ and CD8+ T lymphocytes as well as NK and NKT cells can inhibit hepatocellular replication by a noncytopathic process that is mediated primarily by IFN-γ (8–12, 22). Furthermore, in acutely infected chimpanzees, it has been shown that viral replication is almost completely abolished soon after CD3 and IFN-γ mRNA appear in the liver and that this occurs several weeks before the peak of liver disease (15), suggesting that noncytopathic control of HBV replication may also occur during natural HBV infection. Importantly, HBV-specific peripheral blood T-cell responses and decreases in viremia can be detected before the onset of symptomatic liver disease in patients with acute HBV infection (37), supporting the notion that immune recognition

of infected cells and noncytolytic control of HBV infection may occur during viral hepatitis in humans as well.

Nonetheless, despite the association among the T-cell response, viral clearance, and liver disease during acute HBV infection, a causal relationship among these events has not been proven. Furthermore, the effector cells and effector mechanisms responsible for viral clearance and liver disease during acute HBV infection have not been defined. In addition, the characteristics of the virus-specific T-cell response in the liver during acute HBV infection has never been studied. Thus, nothing is known about the nature, frequency, or function of the intrahepatic T-cell response to HBV or the relationship of that response to the outcome of HBV infection. The present study was performed to address those issues.

MATERIALS AND METHODS

Chimpanzees. Animals were handled according to human use and care guidelines specified by the Animal Research Committees at the National Institutes of Health and the Scripps Research Institute (La Jolla, Calif.). All animals were housed at Bioqual Laboratories (Rockville, Md.), an American Association for Accreditation of Laboratory Animal Care International-accredited institution under contract to the National Institute of Allergy and Infectious Diseases. Three healthy, young adult, HBV-seronegative chimpanzees (chimpanzees 1615, 1620, and 1627) were studied. All animals were inoculated with 10^8 genome equivalents (GE) of a monoclonal HBV (genotype *ayw*) contained in pooled serum from HBV transgenic mice (14). Before inoculation and each week thereafter, blood was obtained by venipuncture and liver tissue was obtained by needle biopsy and shipped to The Scripps Research Institute by overnight express for immunological and virological analysis.

PBMC. Prior to infection and each week thereafter for up to 32 weeks, 40 ml of citric acid-sodium citrate-dextrose anticoagulated blood were obtained for isolation of peripheral blood mononuclear cells (PBMC) and shipped to La Jolla, California, on wet ice for processing the next day. PBMC were isolated on Ficoll-Histopaque density gradients (Sigma Chemical Co., St. Louis, Mo.), washed three times in Hanks balanced salt solution (Gibco Laboratories, Grand Island, N.Y.), and stained for surface markers CD3, CD4, and CD8 immediately. Briefly, 2×10^5 PBMC per well were plated in a 96-well V-bottom plate, stained with the respective antibodies for 30 min on ice, washed three times with phosphate-buffered saline containing 1% fetal calf serum (FCS), and analyzed directly. Fluorescence-activated cell sorter (FACS) analysis was performed at the Scripps Research Institute Flow Cytometry Core Facility by using FACSort and FACScan flow cytometers and analyzed with Cell Quest software (Becton Dickinson, San Jose, Calif.).

* Corresponding author. Mailing address: Department of Molecular and Experimental Medicine, SBR-10, The Scripps Research Institute, 10550 N. Torrey Pines Rd., La Jolla, CA 92037. Phone: (858) 784-8228. Fax: (858) 784-2960. E-mail: fchisari@scripps.edu.
‡ Present address: University of Freiburg, Freiburg, Germany.

Liver biopsy. Prior to infection and each week thereafter, liver tissue was obtained by hepatic needle biopsy. In most instances, two to three tissue fragments 5 to 10 mm in length were obtained. One fragment was immediately placed into RPMI medium (Gibco Laboratories) containing 10% AB serum and cooled on wet ice for shipment to Scripps; another fragment was fixed in 10% zinc formalin solution for subsequent histological examination; and the final fragment was snap frozen for subsequent RNA isolation.

Isolation and expansion of intrahepatic T cells. At weekly intervals, liver-infiltrating lymphocytes were isolated from approximately 0.5 to 1 cm of hepatic needle biopsy sample. The tissue was homogenized in 2 to 3 ml of Dulbecco's phosphate-buffered saline (Gibco Laboratories) with a Dounce tissue grinder. The average number of intrahepatic lymphocytes was between 5×10^4 and 5×10^5 cells. Cell suspensions were then incubated with magnetic beads coupled to either anti-CD8 or anti-CD4 antibodies (Dynabeads; Dynal, Oslo, Norway) for 20 min at 4°C, and bound CD8+ or CD4+ T cells were isolated by using a particle magnetic concentrator. The isolated intrahepatic CD4+ and CD8+ T cells were then plated in separate wells of 24-well plates (Corning, Corning, N.Y.) in 1 ml of 10% human AB+ serum, 100 U of interleukin-2 (IL-2; Hoffmann-La Roche, Inc., Nutley, N.J.)/ml, and 0.04 μg of anti-human CD3 monoclonal antibody (Immunotech, Marseilles, France)/ml as a stimulus to T-cell growth and 2×10^6 irradiated autologous PBMC per well as feeder cells. Twice a week, 1 ml of media was exchanged and 100 U of IL-2/ml was added. After 2 weeks of expansion, 4 to 6 million cells were recovered and the expanded T cells were tested for HBV-specific T-cell responses (see below). The purity of each T-cell subset was always >95%.

Recombinant HBV proteins. A recombinant preparation of hepatitis B core antigen (HBcAg) prepared from bacterial extracts of *Escherichia coli* K-12 strain HB 101 harboring the recombinant plasmid carrying the HBcAg-encoding gene was obtained from Biogen (Cambridge, Mass.) as previously described (29). Purity was over 98% as determined by scanning densitometry of Coomassie blue-stained sodium dodecyl sulfide-polyacrylamide gels.

EBV B-cell lines and recombinant expression vectors. Autologous Epstein-Barr virus (EBV)-transformed B-lymphocyte cell lines (B-LCL) were established as described previously (16). All target cells were maintained in RPMI with 10% (vol/vol) heat-inactivated FCS (Gibco Laboratories). Recombinant vaccinia viruses expressing the HBV core (c-*vac*), polymerase, and large envelope region (*ayw* subtype) have been previously described (16). Wild-type vaccinia viruses were used as a negative control. Briefly, B-LCL were infected at a multiplicity of infection of 25 for 1 h at room temperature with the respective vaccinia viruses. After 1 h, 1 ml of 10% FCS medium was added and the infected B-LCL were cultured (at 37°C) overnight and then washed once before they were added as stimulators to the intracellular IFN-γ staining assays (see below).

Antibodies. Fluorescein isothiocyanate (FITC)-conjugated anti-CD8, phycoerythrin (PE)-conjugated anti-CD8, PE-conjugated anti-CD4, allophycocyanin (APC)-conjugated anti-CD3, PE-conjugated anti-IFN-γ, and FITC-, APC-, or PE-conjugated isotype antibodies were obtained from Pharmingen (San Diego, Calif.) and used for immunostaining and FACS analysis according to the manufacturer's instructions.

CD4+- and CD8+-T-cell depletion. The ability of CD4+ and CD8+ T cells to control HBV infection was monitored in chimpanzees 1615 and 1620, respectively. CD4 depletion was achieved with humanized chimeric monoclonal anti-human CD4 antibody cM-T412, which contains the antigen binding region of a murine antibody, M-T412, and the constant region of a human immunoglobulin G1 κ chain (20). This antibody has been previously used to deplete CD4+ cells in chimpanzees (20) according to a schedule of three intravenous injections of 5 mg/kg of body weight administered once every other day for 1 week. CD8 depletion was performed with a humanized chimeric monoclonal anti-human CD8 antibody cM-T807, which contains the variable region of a murine antibody, M-T807, and the constant region of a human immunoglobulin G1-κ (34, 35). This antibody has been previously used to deplete CD8+ T cells in macaque monkeys (34, 35) according to a schedule of 3 injections of 5 mg/kg over 7 days. Chimpanzee 1627 was treated with an isotype-matched mouse and human chimeric monoclonal antibody directed against respiratory syncytial virus (MedImmune, Inc., Gaithersburg, Md.) as a control.

HBV-specific proliferative T-cell response. Intrahepatic CD4+ T cells were resuspended together with 10^5 autologous irradiated (3,000 rads) PBMCs as APC (10^6 cells/ml) in complete medium with 10% human AB serum, plated at a concentration of 2×10^5 cells/200 μl/well and stimulated with 10 μg of HBcAg/ml or no antigen in five replicate wells of 96-well U-bottom plates. [3H]thymidine (1 μCi; Dupont NEN, Boston, Mass.) was added to each well on day 5. Cultures were harvested on day 6 after 16 h of [3H]thymidine incorporation. The degree of cellular proliferation was expressed as a stimulation index (SI) in which the average [3H]thymidine uptake (in counts per minute) in rep-

licate wells stimulated with HBcAg was divided by the average [3H]thymidine uptake in replicate wells stimulated without antigen. Based on prior analysis of uninfected and infected chimpanzees, an SI of >3.0 was used as a positive cutoff value.

HBV-specific CD8+-T-cell responses. The intrahepatic HBV-specific CD8+-T-cell response was analyzed by intracellular IFN-γ staining of polyclonally expanded CD8+ T lymphocytes (see above) after 5 h of in vitro stimulation with autologous EBV-transformed B-LCL that were infected with recombinant HBV vaccinia viruses that express the HBV envelope, core, and polymerase proteins or with wild-type vaccinia virus as a control. Briefly, previously expanded CD8+ T cells were plated in 96-well plates at 2×10^5 cells per well and stimulated with 2×10^5 cells of autologous EBV-transformed B cells infected with vaccinia viruses that express the HBV envelope, core, or polymerase proteins for 5 h (37°C, 5% CO$_2$) in the presence of 50 U of recombinant human IL-2 (Hoffmann-La Roche)/ml and 1 μg of brefeldin A (Pharmingen)/ml, and then the cells were stained with antibodies to human CD8 and IFN-γ (Pharmingen). Duplicate wells incubated with B-LCLs infected with wild-type vaccinia virus were also included to determine the background level of IFN-γ production. In addition, one well containing only autologous EBV B cells plus CD8+ T cells was included for isotype antibody staining, and another well was stimulated with 10 ng of phorbol 12-myristate 13-acetate (Sigma Chemical Co.)/ml and 200 ng of ionomycin/ml to serve as a positive control for IFN-γ staining. FACS analysis was performed at the Scripps Research Institute Flow Cytometry Core Facility by using FACSort and FACScan flow cytometers and analyzed with Cell Quest software (Becton Dickinson). The frequency of HBV-specific CD8+ T cells was defined as the percentage of CD8+ T cells that produce IFN-γ in response to stimulation by B-LCL coinfected with each of the viral HBV constructs after subtraction of the IFN-γ+ CD8+ T cells detected after stimulation by wild-type vaccinia virus.

RNA isolation and RNase protection assay. Frozen liver tissues were mechanically pulverized, and RNA was extracted by the acid guanidinium-phenol-chloroform method (6). Total RNA (20 μg) was analyzed by the RNase protection assay for quantitation of mRNA exactly as previously described (15).

HBV DNA detection in the liver. Total liver DNA was extracted from liver biopsy samples as described previously (15), and the levels of HBV DNA replicative intermediates were determined by quantitative real-time PCR by using a Bio-Rad iCycler system. Briefly, 10 ng of total liver DNA was subjected to HBV (*ayw*)-specific TaqMan PCR in a 50-μl reaction mixture with TaqMan universal PCR master mix (Applied Biosystems, Foster City, Calif.), 200 nM forward primer HBV469U (5′-CCCGTTTGTCCTCTAATTCC-3′), 200 nM reverse primer HBV569L (5′-GTCCGAAGGTTTGGTACAGC-3′), and 100 nM TaqMan probe HBV495P [5′-6-FAMd(CTCAACAACCAGCACGGGACCA) BHQ-1-3′]. Tenfold serial dilutions (10^8 to 10^0 copies) of plasmid DNA containing a monomeric HBV insert were used as standards in parallel HBV-specific PCRs. In a separate assay, 10 ng of DNA was subjected to quantitative SYBR Green PCR for detection of genomic glyceraldehyde-3-phosphate dehydrogenase (GAPDH) sequences with SYBR Green PCR master mix (Applied Biosystems), 200 nM forward primer GAP4581U (5′-ATTGCCCTCAACGACCAC-3′), and 200 nM reverse primer GAP4661L (5′-GTCTGGCGCCCTCTG-3′). Tenfold serial dilutions (100 ng to 0.1 ng) of human genomic DNA (Clontech, Palo Alto, Calif.) were used as standards in parallel GAPDH-specific PCRs. This protocol allowed for intrahepatic HBV DNA quantification of ≥10 GE/ng of liver DNA.

RESULTS

Course of HBV infection. Three animals were inoculated intravenously with HBV-positive transgenic mouse serum containing 10^8 GE of HBV DNA (*ayw* subtype) that has previously been shown to cause a typical course of acute HBV infection in chimpanzees (15). At the expected time of onset of viremia during week 6 after inoculation, the animals were treated with monoclonal antibodies to human CD4 (chimpanzee 1615), CD8 (chimpanzee 1620), or an irrelevant control antibody (chimpanzee 1627). The virological, immunological, and disease profiles of each animal were monitored on a weekly basis thereafter for the next several months.

Course of HBV infection in the control animal. As shown in Fig. 1A on a linear scale and in Fig. 2A on a logarithmic scale, hepatic HBV DNA levels became detectable in chimpanzee
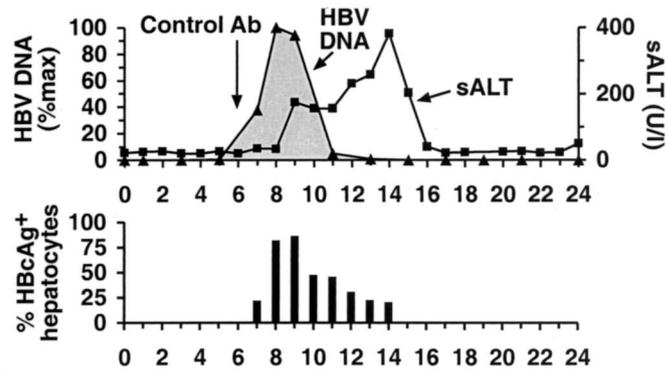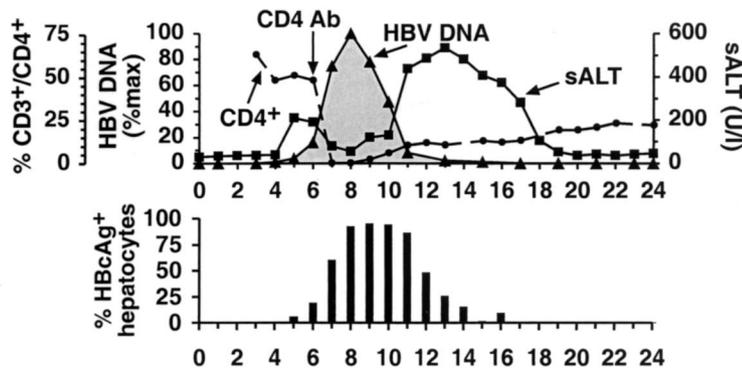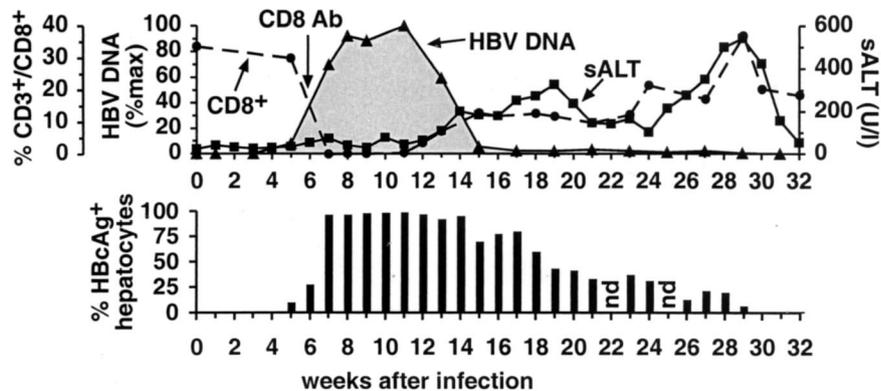
FIG. 1. Course of acute HBV infection in chimpanzees after experimental inoculation with HBV in the presence or absence of CD4^{+} and CD8^{+} cells. All animals were inoculated with 10^8 GE of HBV intravenously in week 0 and with a monoclonal antibody (see below) in week 6. (A) Chimpanzee (Ch.) 1627 was injected with irrelevant control antibody (Ab). (B) Chimpanzee 1615 was injected with a CD4-specific monoclonal antibody. (C) Chimpanzee 1620 was injected with a CD8-specific monoclonal antibody. Intrahepatic HBV DNA (black triangles) is expressed as a percentage (%max) of the corresponding peak HBV DNA levels in the liver of each animal. sALT activity (black squares) is expressed in units per liter. HBcAg-positive hepatocytes are expressed as a percentage of the total number of hepatocytes. The number of CD3^{+} CD4^{+} or CD3^{+} CD8^{+} T cells is expressed as a percentage of the total number of CD3^{+} T cells in the peripheral blood. Vertical arrows indicate the time of antibody treatment.

1627 by quantitative PCR during week 5 after inoculation when the intrahepatic HBV DNA content was 249 GE/ng of liver DNA and approximately 0.2% of the hepatocytes were HBcAg positive. The intrahepatic content of HBV DNA peaked at 3.9×10^4 copies/ng of liver DNA in week 8, at which time 82% of the hepatocytes were HBcAg positive. Based on these figures, there were approximately 285 HBV DNA molecules per infected hepatocyte, or 1.3×10^{13} GE of HBV in the
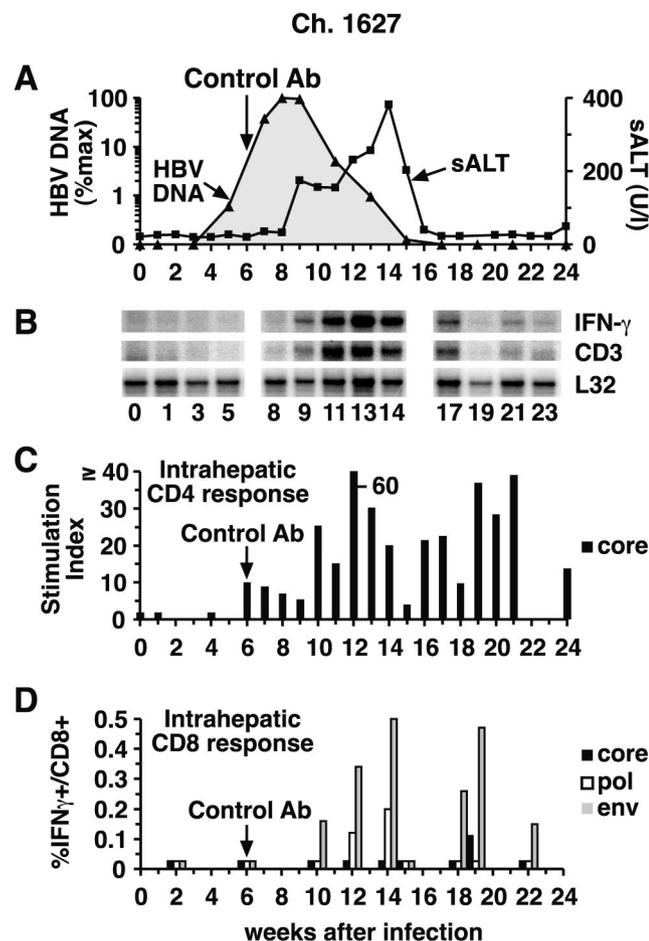
Ch. 1627

FIG. 2. Intrahepatic cytokine profile and HBV-specific T-cell responses during acute HBV infection in control chimpanzee (Ch.) 1627. (A) The courses of intrahepatic HBV DNA and sALT activity during acute infection are displayed as described in the legend to Fig. 1, except for the intrahepatic HBV DNA content, which is displayed on a logarithmic scale in this figure and in Fig. 3 and 4 in order to facilitate comparison of the duration of the infection in the 3 animals. (B) Total RNA isolated from liver biopsy samples was analyzed for the expression of CD3, IFN-γ, and L32 by an RNase protection assay. The L32 signals reflect the amount of RNA used in the assay. (C) The intrahepatic CD4+-T-cell response to HBcAg is expressed as the SI. (D) The intrahepatic CD8+-T-cell response is shown as the percentage of intrahepatic CD8+ cells that produce IFN-γ after stimulation with autologous EBV B cells that were infected with recombinant vaccinia viruses expressing the HBV core, polymerase, and large envelope proteins after subtraction of their responsiveness to the same B cells infected by wild-type vaccinia virus. The vertical arrow indicates control antibody (Ab) treatment.
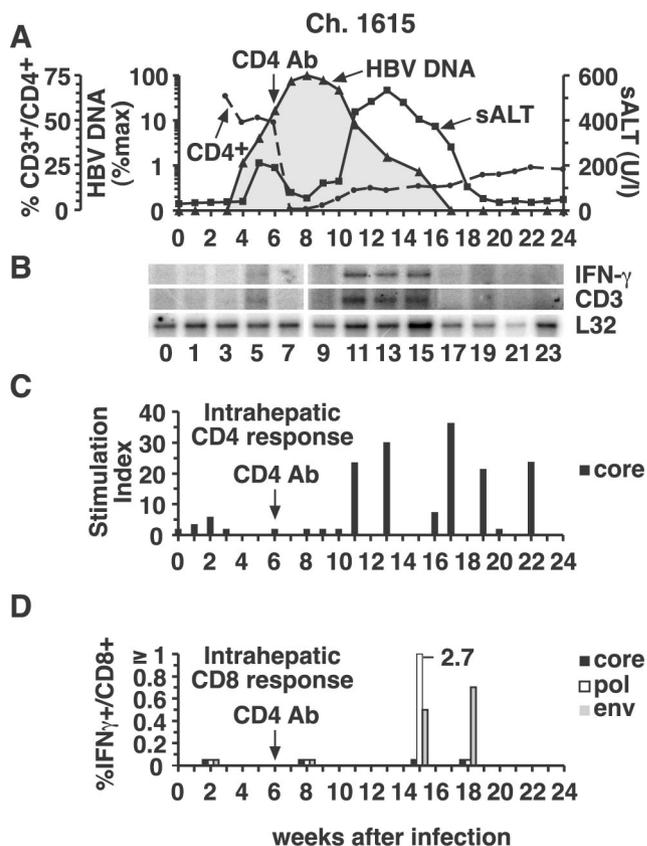
Ch. 1615

FIG. 3. Intrahepatic cytokine profile and HBV-specific T-cell responses during acute HBV infection and CD4 depletion in chimpanzee (Ch.) 1615. (A) The courses of intrahepatic HBV DNA and sALT activity during acute infection and CD4 depletion are displayed as described in the legend to Fig. 2A. (B) Analysis of intrahepatic CD3, IFN-γ, and L32 expression. (C) The intrahepatic CD4+-T-cell response to HBcAg during acute infection and CD4 depletion. (D) Intrahepatic CD8+-T-cell responses during acute infection and CD4 depletion. See the legend to Fig. 2 for all other details. Ab, antibody.

liver at that time point, representing a >133,000-fold amplification of the inoculum at the peak of the infection. Between weeks 8 and 11, the HBV DNA content of the liver abruptly decreased by more than 95% while the fraction of HBcAg-positive hepatocytes fell by less than 40% and there was only a slight increase in serum alanine amino transferase (sALT) activity. Subsequently, however, sALT activity increased, reached a peak of 381 U/liter by week 14, and returned rapidly to the baseline by week 17. This delayed episode of liver disease coincided with the final elimination of HBV DNA and HBcAg-positive hepatocytes from the liver at week 17. It is

noteworthy that all of these events occurred in the absence of an anti-HBs antibody response, which was not detected until week 26 (not shown), long after viral clearance had occurred.

Depletion of CD4+ cells does not alter the duration or outcome of acute HBV infection. As shown in Fig. 1B and 3A, the course of infection in chimpanzee 1615 was almost identical to that in chimpanzee 1627, despite the fact that chimpanzee 1615 was depleted of CD4+ cells in week 6 after infection, at which time hepatic HBV DNA levels were rapidly rising. Unexpectedly, a small peak of sALT activity was detectable in this animal during the period of logarithmic viral expansion prior to CD4 depletion. Interestingly, circulating CD4+ cells became undetectable, and the early sALT peak subsided in parallel with CD4 depletion (Fig. 1B, week 7), suggesting that CD4+ cells may have contributed to the atypically early liver disease in this animal. The absence of CD4+ cells, however, didn't affect the rate of viral spread or the magnitude of the infection. Specifically, HBV DNA levels peaked at 2.7×10^4 copies/ng of liver DNA in week 8, at which time 92.5% of hepatocytes were HBcAg positive, reflecting the presence of about 175 copies of HBV DNA per infected cell or 9.3×10^{12}
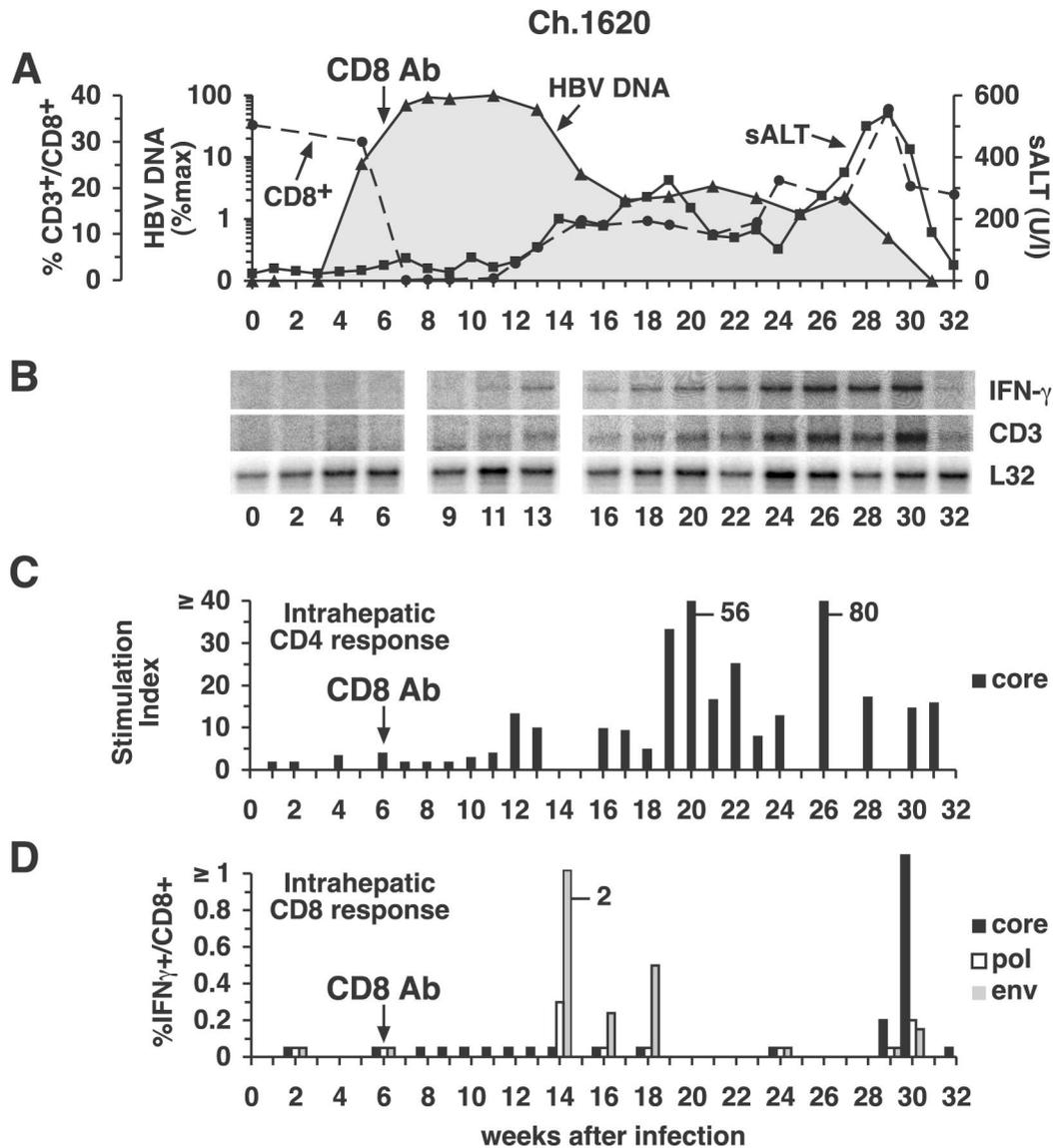
FIG. 4. Intrahepatic cytokine profile and HBV-specific T-cell responses during acute HBV infection and CD8 depletion in chimpanzee (Ch.) 1620. (A) The courses of intrahepatic HBV DNA and sALT activity during acute infection and CD8 depletion are displayed as described in the legend to Fig. 2A. (B) Analysis of intrahepatic CD3, IFN-γ, and L32 expression. (C) The intrahepatic CD4+-T-cell response to HBcAg during acute infection and CD8 depletion. (D) Intrahepatic CD8+-T-cell responses during acute infection and CD8 depletion. See the legend to Fig. 2 for all other details. Ab, antibody.

GE of HBV in the entire liver, i.e., slightly lower than that in the control animal at the same time point. Like in the control animal, the hepatic HBV DNA levels fell by >90% between weeks 8 and 11, coincident with the return of CD4+ cells to the circulation, while the level of HBcAg-positive hepatocytes decreased less than 7% and there was a slight increase in sALT activity. Subsequently, the sALT activity rose, reached a peak of 534 U/liter in week 13, and returned to baseline by week 19, 2 weeks after the disappearance of HBV DNA from the liver, coinciding with the disappearance of HBcAg-positive hepatocytes and the absence of an anti-HBs antibody response which was not detectable until week 32 after inoculation (data not shown). It is important to emphasize that the profound decrease in HBV DNA between weeks 8 and 11 occurred as

CD4+ T cells reappeared, but the dynamic changes in sALT activity during weeks 10 to 19 occurred even though the number of circulating CD4+ cells was less than 23% of the baseline level and relatively stable at that time. It is also important to note that the number of peripheral CD8+ cells did not change during the period of profound CD4 depletion (data not shown). Thus, the course of HBV infection was almost identical in the control and CD4-depleted animals, both of whose CD8+-T-cell populations were intact.

Depletion of CD8+ cells dramatically alters the duration and outcome of acute HBV infection. As shown in Fig. 1C and 4A, chimpanzee 1620 was treated with a monoclonal anti-CD8 antibody during week 6, when HBV DNA levels were rapidly rising in the liver. During the infusion, the CD8+ cells imme-

diately became undetectable, and they didn't begin to reappear until week 12 when they started a slow, prolonged, and somewhat halting recovery. Despite the CD8⁺ cell depletion, the early kinetics of the infection, until week 8, were almost indistinguishable from those in the control and CD4-depleted animals. Indeed, at week 8, 96% of the hepatocytes were HBcAg positive and HBV DNA replicative intermediates were present at a level of 3.3×10^4 GE/ng of liver DNA, reflecting 207 copies per hepatocyte or 1.3×10^{13} copies in the entire liver, almost identical to the number of copies in control chimpanzee 1627 (Fig. 1A).

Subsequently, however, the virological and pathogenic events in the CD8-depleted chimpanzee were vastly different from those in the control and CD4-depleted animals. As illustrated in Fig. 1C and especially in Fig. 4A, which replots the course of infection on a logarithmic scale in order to display the virological changes after week 15 when HBV DNA levels were very low, there was a striking relationship between the number of circulating CD8⁺ cells and both virus titer and sALT activity at the later time points in the infection. For example, in the absence of CD8⁺ cells, the time span of peak infection (weeks 8 to 11) was prolonged, the time of onset of the initial decrease in HBV DNA levels and increase in sALT activity (week 13) was delayed, and the time required for the first phase of viral clearance (week 15) and the eventual termination of infection (week 31) were markedly delayed and prolonged. Importantly, the total intrahepatic HBV DNA content and the number of HBV DNA GE per hepatocyte remained at their initial peak levels until week 11, i.e., for as long as CD8⁺ cells were undetectable in the circulation. The reappearance of CD8⁺ cells between weeks 11 and 17 was associated with the onset of a mild liver disease and with a 50-fold reduction in total liver HBV DNA to 2.5×10^{11} copies in the entire liver, even though the number of HBcAg-positive hepatocytes decreased only 18% during the same time period, suggesting that, as in the previous two animals, HBV replication was inhibited noncytopathically at this stage of the infection.

Surprisingly, after their initial recovery, the number of CD8⁺ cells stabilized at approximately 40% of baseline levels between weeks 16 to 27, and this was associated with a comparably stable plateau in sALT activity and intrahepatic HBV DNA content (Fig. 1C and 4A). In contrast, the number of HBcAg-positive hepatocytes decreased progressively in the same time period despite a stable total HBV DNA content of 2.8×10^{11} copies in the entire liver on week 27. These results, together with the absence of serum anti-HBs antibodies in this animal until weeks 42 to 45 (data not shown), suggest that HBcAg-positive hepatocytes apparently were being destroyed and replaced during this prolonged period of time, yet the infection wasn't eliminated, presumably because of unopposed viral spread to new hepatocytes. Unexpectedly, on week 29, the number of CD8⁺ cells suddenly rebounded to baseline levels, and this coincided with a surge in sALT activity and the disappearance of HBV DNA from the liver. As in the previous animals, all of these events occurred in the absence of anti-HBs neutralizing antibodies (data not shown), suggesting that viral clearance could be attributed to the effects of the CD8⁺ cells in this animal. It is also important to note that the number of peripheral CD4⁺ cells remained normal during the period of profound CD8 depletion when the infection was greatly pro-

longed, further supporting the notion that the virological events in this animal were CD8 dependent.

Intrahepatic T-cell and cytokine profiles during acute HBV infection. In order to determine the extent to which the foregoing virological and pathogenic events were related to the adaptive intrahepatic T-cell response to HBV, we studied the magnitude and kinetics of the HBV-specific CD4⁺- and CD8⁺-T-cell response at multiple time points in these animals. In addition, total liver RNA was subjected to RNase protection analysis in order to monitor changes in global T-cell and cytokine gene expression in the liver.

Control animal chimpanzee 1627. As shown in Fig. 2C, an intrahepatic HBcAg-specific CD4⁺-T-cell response was first detectable in chimpanzee 1627 in week 6 and it surged by week 10 to levels that were, for the most part, sustained for the duration of the study. Importantly, the onset of the CD4⁺-T-cell response was not associated with a decrease in the HBV DNA titer or an increase in sALT activity (Fig. 2A). In contrast, HBV DNA levels started to decrease, and sALT activity started to rise, when HBV envelope-specific CD8⁺ T cells became detectable in the liver on week 10 (Fig. 2D), and there was a corresponding surge in the intrahepatic CD4⁺-T-cell response (Fig. 2C) and the appearance of CD3 and IFN-γ mRNA (Fig. 2B) in the liver. The intrahepatic CD8⁺-T-cell response persisted, strengthened, and diversified to include HBV core and polymerase specificities over the next several weeks (Fig. 2D), as did the intrahepatic content of CD3 and IFN-γ mRNA (Fig. 2B), until viral DNA was no longer detectable and sALT activity returned to normal in week 17 (Fig. 2A). Interestingly, HBV-specific CD4 and CD8⁺-T-cell responses remained easily detectable in the liver for at least several weeks after viral clearance, implying that traces of virus may persist after apparent eradication of the infection.

CD4-depleted animal chimpanzee 1615. As shown in Fig. 3C, the intrahepatic HBcAg-specific CD4⁺-T-cell response wasn't detectable in the CD4-depleted chimpanzee 1615 until week 11, at which time the total HBV DNA content of the liver had already decreased by more than 92% and sALT activity had already started to rise (Fig. 3A), suggesting that CD4⁺ T cells did not play an effector role in these events. Unfortunately, we were unable to expand the intrahepatic CD8⁺-T-cell population between week 8 (when HBV-specific CD8⁺ T cells were undetectable) and week 15 (when they were strongly positive) (Fig. 3D), so we can't determine whether the changing virological and pathological status of the animal during that period was temporally related to the CD8⁺-T-cell response. Between weeks 11 and 18, however, HBV-specific CD4⁺ (Fig. 3C) and CD8⁺ T cells (Fig. 3D) were detectable in the liver, corresponding with the appearance of CD3 and IFN-γ mRNA (Fig. 3B), the peak of liver disease, and the final elimination of detectable viral DNA (Fig. 3A).

CD8-depleted animal chimpanzee 1620. As shown in Fig. 4A, the virus titer remained at peak levels and didn't start to fall in CD8-depleted chimpanzee 1620 until week 13, i.e., 1 week after CD8⁺ T cells reappeared in the circulation, and coincident with the appearance of HBV-specific, IFN-γ-producing CD8⁺ T cells in the liver (Fig. 4D), suggesting a causal relationship between the two events. The appearance of HBcAg-specific CD4⁺ T cells in the liver was also delayed in this animal even though the total number of circulating CD4⁺

T cells was unaffected by CD8 depletion, suggesting that the accumulation of HBV-specific CD4$^+$ T cells in the liver might be CD8 dependent. Interestingly, between weeks 16 and 30, the intrahepatic content of CD3 and IFN-γ mRNA progressively increased (Fig. 4B), especially between weeks 24 and 30, apparently reflecting the accumulation of virus-specific T cells in the liver (Fig. 4C and D). Note that the surge in intrahepatic CD3 and IFN-γ mRNA content (Fig. 4B) was associated with a surge in the HBV-specific T-cell response (Fig. 4C and D), an increase in the severity of the liver disease (Fig. 4A), and elimination of detectable virus DNA (Fig. 4A).

DISCUSSION

The results of this study illustrate several new and important aspects of the HBV-specific T-cell response during acute HBV infection. First, we demonstrated that approximately 220 ± 56 GE of HBV DNA are present in each infected hepatocyte and that virtually all hepatocytes are infected at the peak of HBV infection, representing a viral load of approximately $1.1 \times 10^{13} \pm 0.2 \times 10^{13}$ GE in the infected liver.

Second, we observed that viral clearance involves two distinct processes, one of which is noncytolytic and may produce a >50-fold decrease in total liver HBV DNA, which reduces the total viral load to approximately 10^{11} GE in the infected liver. If there are approximately 5×10^{10} hepatocytes in a chimpanzee liver, this translates either to a uniform reduction of infection that leaves all of the hepatocytes infected at a level of approximately 2 to 4 GE per cell or to complete elimination of the virus from 98 to 99% of the hepatocytes, with no change in the level of infection in the rest. The first hypothesis might appear more tenable at first glance, since we observed the virus DNA level to decrease without a corresponding decrease in the number of HBcAg-positive hepatocytes. The second hypothesis is equally possible, however, because the HBcAg-positive hepatocytes were quantitated in this study by counting the number of cells whose nuclei contain HBcAg. We have previously shown that HBcAg particles do not disappear from the nucleus until the cell divides, even though viral replication and gene expression are extinguished (13); and we have recently shown that, in the absence of cell division, HBcAg particles are stable in the nucleus for many months in the absence of HBcAg synthesis (unpublished data). Thus, both hypotheses are tenable at this point, and more work is needed to make this important distinction.

Third, we showed that viral clearance initially coincided with the appearance of HBV-specific CD4$^+$ and CD8$^+$ T cells as well as CD3 mRNA and IFN-γ mRNA in the liver and that it occurred without a commensurate degree of hepatitis, suggesting that viral replication is inhibited noncytopathically at this point in the infection and that IFN-γ produced by the HBV-specific T cells may have been responsible. The potential role of IFN-γ is supported by results from our laboratory demonstrating that the intrahepatic induction of this cytokine by various stimuli can inhibit HBV replication in the livers of HBV transgenic mice (10). In addition, results from our laboratory previously demonstrated the same phenomena in a well-differentiated, continuous hepatocyte cell line that replicates HBV (28).

Fourth, the data suggest that CD8$^+$ cells are required for the control of HBV since CD8 depletion in chimpanzee 1620 greatly prolonged the infection and delayed the onset of viral clearance and liver disease until CD8$^+$ T cells reappeared in the circulation and virus-specific CD8$^+$ T cells entered the liver. In contrast, the duration of infection was unaffected by CD4 depletion. Importantly, all of these events coincided with the appearance of HBV-specific T cells and the induction of both CD3 and IFN-γ mRNA in the liver. Thus, we conclude that CD8$^+$ cells contribute importantly to the noncytolytic control of HBV replication in the liver of infected animals and also to the cytolytic process that regularly accompanies viral clearance.

Fifth, our results suggest that CD4$^+$ cells probably don't function as effector cells in the control of HBV since the depletion of CD4$^+$ cells in chimpanzee 1615 had little or no effect on the duration of the infection (Fig. 1B and 3A). Indeed, inspection of Fig. 1 reveals that, compared to control chimpanzee 1627 (Fig. 1A and 2A), CD4$^+$ cell depletion in chimpanzee 1615 (Fig. 1B and 2A) did not have a significant effect on the time required to achieve peak virus titer (8 weeks) or the time required to eliminate HBV DNA from the liver (15 weeks). Furthermore, the massive reduction in HBV DNA that occurred between weeks 8 and 10 in chimpanzee 1615 (Fig. 1B and 3A) occurred in the absence of a detectable HBV-specific intrahepatic CD4$^+$-T-cell response (Fig. 3C), arguing against an effector role for these cells during the early phase of virus control. This argument is supported by the unchanging virus load in control chimpanzee 1627 between weeks 6 and 9 of infection (Fig. 1A and 2A), despite the emergence of an intrahepatic HBV-specific CD4$^+$-T-cell response during that time period (Fig. 2C). It is further supported by the occurrence of a 50-fold reduction in hepatic HBV DNA content between weeks 10 and 17 in chimpanzee 1620 (Fig. 1C and 4A) in the context of a low level and unchanging intrahepatic CD4$^+$-T-cell response during the same interval (Fig. 4C). In contrast, the massive reduction in virus DNA in the liver of chimpanzees 1627 and 1620 (Fig. 2A and 4A) was accompanied by the onset of an intrahepatic HBV-specific CD8$^+$-T-cell response in both animals (Fig. 2D and 4D). Interestingly, however, CD4$^+$ T cells may have played an effector role in the atypically early onset of liver disease that preceded CD4 depletion during week 6 in chimpanzee 1615 because it was temporally associated with a fall in sALT activity in weeks 7 and 8, a rise in sALT activity in parallel with the reappearance of circulating CD4$^+$ T cells in week 9 (Fig. 3A), and a surge in sALT activity in week 11 (Fig. 3A), when intrahepatic CD4$^+$ T cells first appeared (Fig. 3A and C). Arguing against this hypothesis, however, is the absence of detectable CD4$^+$ T cells in the liver during week 6 (Fig. 3C). Nonetheless, because of their central role as regulators of the immune response, we presume that CD4$^+$ T cells are essential for the control of HBV infection by facilitating the induction and maintenance of the CD8$^+$-T-cell response, as has been shown in other virus systems (1, 23, 26). Indeed, the slightly prolonged duration of liver disease in chimpanzee 1615 (Fig. 1B and 3A) relative to that in control chimpanzee 1627 (Fig. 1A) may reflect the impact of CD4 depletion in this animal. Our failure to demonstrate a more convincing role for CD4$^+$ T cells was probably due to the fact that they weren't eliminated until week 6 after inoculation, at which time their immunoregulatory role had already been per-

formed, and subsequent events could continue relatively normally in their absence. Additional studies, perhaps involving CD4$^+$-T-cell depletion prior to inoculation, are needed to test this hypothesis.

Finally, the data suggest that cytolytic events are also required for complete elimination of HBV from the liver, as suggested by previous studies with woodchucks (17, 21) and ducks (18, 19) infected with the corresponding hepadnaviruses. This observation was possible because, following CD8 depletion in chimpanzee 1620, the recovery of peripheral CD8$^+$ cells unexpectedly stalled, thereby affording an unusual opportunity to observe the viral dynamics in the context of a subnormal number of CD8$^+$ T cells. Impressively, the intrahepatic HBV DNA content and sALT activity level remained at a relatively stable plateau as long as the total peripheral CD8$^+$-T-cell count was also stable (Fig. 1C and 4A). Nonetheless, there was continuous biochemical evidence of liver cell injury, and this was accompanied by a progressive decrease in the number of HBcAg-positive hepatocytes (Fig. 1C), implying that death and turnover of infected hepatocytes was occurring during this period. These results suggest that, in contrast to the apparent ease with which >98% of the virus DNA was eliminated from the liver when CD8$^+$ T cells reappeared in this animal, it was relatively difficult to completely eliminate the infection when the CD8$^+$-T-cell count was suppressed, presumably because the virus was not completely eliminated and, in the absence of neutralizing antibodies, it could continue to spread to new hepatocytes. Since the final clearance of the virus in chimpanzee 1620 coincided precisely with a surge in sALT activity (Fig. 1C and 4A), and since both of those parameters coincided with the return of peripheral CD8$^+$ cells to baseline levels (Fig. 1C and 4A), a surge in the intrahepatic HBV-specific CD8$^+$-T-cell response (Fig. 4D), and a surge in intrahepatic IFN-γ mRNA content (Fig. 4B), it would appear that CD8 T-cell-mediated cytolytic and noncytolytic functions both contribute to the final elimination of the virus.

Thus, our results demonstrate that intrahepatic HBV-specific CD8$^+$ T cells are required for rapid viral clearance during acute HBV infection. In addition, the data suggest the existence of dual antiviral functions that overlap temporally during natural acute HBV infection but can be clearly separated by CD8 depletion: a primarily noncytolytic CD8-dependent mechanism that may be mediated by the secretion of IFN-γ and a primarily cytolytic mechanism that clears the remaining infected cells. We do not know if the two mechanisms are performed by the same or different CD8$^+$ populations. Additional experiments are needed to answer this question and to examine the immunoregulatory role of the CD4$^+$-T-cell response early in the infection.

REFERENCES

1. **Battegay, M., D. Moskophidis, A. Rahemtulla, H. Hengartner, T. W. Mak, and R. M. Zinkernagel.** 1994. Enhanced establishment of a virus carrier state in adult CD4$^+$ T-cell-deficient mice. J. Virol. **68:**4700–4704.
2. **Bertoletti, A., M. M. D'Elios, C. Boni, M. De Carli, A. L. Zignego, M. Durazzo, G. Missale, A. Penna, F. Fiaccadori, G. Del Prete, and C. Ferrari.** 1997. Different cytokine profiles of intrahepatic T cells in chronic hepatitis B and hepatitis C virus infections. Gastroenterology **112:**193–199.
3. **Bertoletti, A., C. Ferrari, F. Fiaccadori, A. Penna, R. Margolskee, H. J. Schlicht, P. Fowler, S. Guilhot, and F. V. Chisari.** 1991. HLA class I-restricted human cytotoxic T cells recognize endogenously synthesized hepatitis B virus nucleocapsid antigen. Proc. Natl. Acad. Sci. USA **88:**10445–10449.
4. **Bertoni, R., A. Sette, J. Sidney, L. G. Guidotti, M. Shapiro, R. Purcell, and F. V. Chisari.** 1998. Human class I supertypes and CTL repertoires extend to chimpanzees. J. Immunol. **161:**4447–4455.
5. **Chisari, F. V.** 2000. Rous-Whipple award lecture. Viruses, immunity, and cancer: lessons from hepatitis B. Am. J. Pathol. **156:**1117–1132.
6. **Chomczynski, P., and N. Sacchi.** 1987. Single-step method of RNA isolation by acid guanidinium thiocyanate-phenol-chloroform extraction. Anal. Biochem. **162:**156–159.
7. **Ferrari, C., A. Penna, T. Giuberti, M. J. Tong, E. Ribera, F. Fiaccadori, and F. V. Chisari.** 1987. Intrahepatic, nucleocapsid antigen-specific T cells in chronic active hepatitis B. J. Immunol. **139:**2050–2058.
8. **Franco, A., L. G. Guidotti, M. V. Hobbs, V. Pasquetto, and F. V. Chisari.** 1997. Pathogenetic effector function of CD4-positive T helper 1 cells in hepatitis B virus transgenic mice. J. Immunol. **159:**2001–2008.
9. **Guidotti, L. G., K. Ando, M. V. Hobbs, T. Ishikawa, L. Runkel, R. D. Schreiber, and F. V. Chisari.** 1994. Cytotoxic T lymphocytes inhibit hepatitis B virus gene expression by a noncytolytic mechanism in transgenic mice. Proc. Natl. Acad. Sci. USA **91:**3764–3768.
10. **Guidotti, L. G., and F. V. Chisari.** 2000. Cytokine-mediated control of viral infections. Virology **273:**221–227.
11. **Guidotti, L. G., and F. V. Chisari.** 2001. Noncytolytic control of viral infections by the innate and adaptive immune response. Annu. Rev. Immunol. **19:**65–91.
12. **Guidotti, L. G., T. Ishikawa, M. V. Hobbs, B. Matzke, R. Schreiber, and F. V. Chisari.** 1996. Intracellular inactivation of the hepatitis B virus by cytotoxic T lymphocytes. Immunity **4:**25–36.
13. **Guidotti, L. G., V. Martinez, Y. T. Loh, C. E. Rogler, and F. V. Chisari.** 1994. Hepatitis B virus nucleocapsid particles do not cross the hepatocyte nuclear membrane in transgenic mice. J. Virol. **68:**5469–5475.
14. **Guidotti, L. G., B. Matzke, H. Schaller, and F. V. Chisari.** 1995. High-level hepatitis B virus replication in transgenic mice. J. Virol. **69:**6158–6169.
15. **Guidotti, L. G., R. Rochford, J. Chung, M. Shapiro, R. Purcell, and F. V. Chisari.** 1999. Viral clearance without destruction of infected cells during acute HBV infection. Science **284:**825–829.
16. **Guilhot, S., P. Fowler, G. Portillo, R. F. Margolskee, C. Ferrari, A. Bertoletti, and F. V. Chisari.** 1992. Hepatitis B virus (HBV)-specific cytotoxic T-cell response in humans: production of target cells by stable expression of HBV-encoded proteins in immortalized human B-cell lines. J. Virol. **66:**2670–2678.
17. **Guo, J. T., H. Zhou, C. Liu, C. Aldrich, J. Saputelli, T. Whitaker, M. I. Barrasa, W. S. Mason, and C. Seeger.** 2000. Apoptosis and regeneration of hepatocytes during recovery from transient hepadnavirus infections. J. Virol. **74:**1495–1505.
18. **Jilbert, A. R., J. A. Botten, D. S. Miller, E. M. Bertram, P. M. Hall, J. Kotlarski, and C. J. Burrell.** 1998. Characterization of age- and dose-related outcomes of duck hepatitis B virus infection. Virology **244:**273–282.
19. **Jilbert, A. R., T. T. Wu, J. M. England, P. M. Hall, N. Z. Carp, A. P. O'Connell, and W. S. Mason.** 1992. Rapid resolution of duck hepatitis B virus infections occurs after massive hepatocellular involvement. J. Virol. **66:**1377–1388.
20. **Jonker, M., W. Slingerland, G. Treacy, P. van Eerd, K. Y. Pak, E. Wilson, S. Tam, K. Bakker, A. F. Lobuglio, P. Rieber, et al.** 1993. In vivo treatment with a monoclonal chimeric anti-CD4 antibody results in prolonged depletion of circulating CD4+ cells in chimpanzees. Clin. Exp. Immunol. **93:**301–307.
21. **Kajino, K., A. R. Jilbert, J. Saputelli, C. E. Aldrich, J. Cullen, and W. S. Mason.** 1994. Woodchuck hepatitis virus infections: very rapid recovery after a prolonged viremia and infection of virtually every hepatocyte. J. Virol. **68:**5792–5803.
22. **Kakimi, K., L. G. Guidotti, Y. Koezuka, and F. V. Chisari.** 2000. Natural killer T cell activation inhibits hepatitis B virus replication in vivo. J. Exp. Med. **192:**921–930.
23. **Kalams, S. A., and B. D. Walker.** 1998. The critical need for CD4 help in maintaining effective cytotoxic T lymphocyte responses. J. Exp. Med. **188:**2199–2204.
24. **Maini, M. K., C. Boni, C. K. Lee, J. R. Larrubia, S. Reignat, G. S. Ogg, A. S. King, J. Herberg, R. Gilson, A. Alisa, R. Williams, D. Vergani, N. V. Naoumov, C. Ferrari, and A. Bertoletti.** 2000. The role of virus-specific CD8$^+$ cells in liver damage and viral control during persistent hepatitis B virus infection. J. Exp. Med. **191:**1269–1280.

25. **Maini, M. K., C. Boni, G. S. Ogg, A. S. King, S. Reignat, C. K. Lee, J. R. Larrubia, G. J. Webster, A. J. McMichael, C. Ferrari, R. Williams, D. Vergani, and A. Bertoletti.** 1999. Direct ex vivo analysis of hepatitis B virus-specific CD8$^+$ T cells associated with the control of infection. Gastroenterology **117:**1386–1396.

26. **Matloubian, M., R. J. Concepcion, and R. Ahmed.** 1994. CD4$^+$ T cells are required to sustain CD8$^+$ cytotoxic T-cell responses during chronic viral infection. J. Virol. **68:**8056–8063.

27. **Missale, G., A. Redeker, J. Person, P. Fowler, S. Guilhot, H. J. Schlicht, C. Ferrari, and F. V. Chisari.** 1993. HLA-A31- and HLA-Aw68-restricted cytotoxic T cell responses to a single hepatitis B virus nucleocapsid epitope during acute viral hepatitis. J. Exp. Med. **177:**751–762.

28. **Pasquetto, V., S. F. Wieland, S. L. Uprichard, M. Tripodi, and F. V. Chisari.** 2002. Cytokine-sensitive replication of hepatitis B virus in immortalized mouse hepatocyte cultures. J. Virol. **76:**5646–5653.

29. **Penna, A., M. Artini, A. Cavalli, M. Levrero, A. Bertoletti, M. Pilli, F. V. Chisari, B. Rehermann, G. Del Prete, F. Fiaccadori, and C. Ferrari.** 1996. Long-lasting memory T cell responses following self-limited acute hepatitis B. J. Clin. Investig. **98:**1185–1194.

30. **Rehermann, B.** 2000. Intrahepatic T cells in hepatitis B: viral control versus liver cell injury. J. Exp. Med. **191:**1263–1268.

31. **Rehermann, B., K. M. Chang, J. McHutchinson, R. Kokka, M. Houghton, C. M. Rice, and F. V. Chisari.** 1996. Differential cytotoxic T-lymphocyte responsiveness to the hepatitis B and C viruses in chronically infected patients. J. Virol. **70:**7092–7102.

32. **Rehermann, B., P. Fowler, J. Sidney, J. Person, A. Redeker, M. Brown, B. Moss, A. Sette, and F. V. Chisari.** 1995. The cytotoxic T lymphocyte response to multiple hepatitis B virus polymerase epitopes during and after acute viral hepatitis. J. Exp. Med. **181:**1047–1058.

33. **Rehermann, B., D. Lau, J. H. Hoofnagle, and F. V. Chisari.** 1996. Cytotoxic T lymphocyte responsiveness after resolution of chronic hepatitis B virus infection. J. Clin. Investig. **97:**1655–1665.

34. **Schmitz, J. E., M. J. Kuroda, S. Santra, V. G. Sasseville, M. A. Simon, M. A. Lifton, P. Racz, K. Tenner-Racz, M. Dalesandro, B. J. Scallon, J. Ghrayeb, M. A. Forman, D. C. Montefiori, E. P. Rieber, N. L. Letvin, and K. A. Reimann.** 1999. Control of viremia in simian immunodeficiency virus infection by CD8+ lymphocytes. Science **283:**857–860.

35. **Schmitz, J. E., M. A. Simon, M. J. Kuroda, M. A. Lifton, M. W. Ollert, C. W. Vogel, P. Racz, K. Tenner-Racz, B. J. Scallon, M. Dalesandro, J. Ghrayeb, E. P. Rieber, V. G. Sasseville, and K. A. Reimann.** 1999. A nonhuman primate model for the selective elimination of CD8+ lymphocytes using a mouse-human chimeric monoclonal antibody. Am. J. Pathol. **154:**1923–1932.

36. **Thimme, R., K. M. Chang, J. Pemberton, A. Sette, and F. V. Chisari.** 2001. Degenerate immunogenicity of an HLA-A2-restricted hepatitis B virus nucleocapsid cytotoxic T-lymphocyte epitope that is also presented by HLA-B51. J. Virol. **75:**3984–3987.

37. **Webster, G. J., S. Reignat, M. K. Maini, S. A. Whalley, G. S. Ogg, A. King, D. Brown, P. L. Amlot, R. Williams, D. Vergani, G. M. Dusheiko, and A. Bertoletti.** 2000. Incubation phase of acute hepatitis B in man: dynamic of cellular immune mechanisms. Hepatology **32:**1117–1124.